© 2018. Published by The Company of Biologists Ltd | Journal of Cell Science (2018) 131, jcs210989. doi:10.1242/jcs.210989

RESEARCH ARTICLE

Maturation of neural stem cells and integration into hippocampal circuits – a functional study in an *in situ* model of cerebral ischemia

Olga Kopach[1,2,*], Oksana Rybachuk[1,3], Volodymyr Krotov[1], Vitalii Kyryk[3], Nana Voitenko[1,4] and Tatyana Pivneva[1,3,4]

ABSTRACT

The hippocampus is the region of the brain that is most susceptible to ischemic lesion because it contains pyramidal neurons that are highly vulnerable to ischemic cell death. A restricted brain neurogenesis limits the possibility of reversing massive cell death after stroke and, hence, endorses cell-based therapies for neuronal replacement strategies following cerebral ischemia. Neurons differentiated from neural stem/progenitor cells (NSPCs) can mature and integrate into host circuitry, improving recovery after stroke. However, how the host environment regulates the NSPC behavior in post-ischemic tissue remains unknown. Here, we studied functional maturation of NSPCs in control and post-ischemic hippocampal tissue after modelling cerebral ischemia *in situ*. We traced the maturation of electrophysiological properties and integration of the NSPC-derived neurons into the host circuits, with these cells developing appropriate activity 3 weeks or less after engraftment. In the tissue subjected to ischemia, the NSPC-derived neurons exhibited functional deficits, and differentiation of embryonic NSPCs to glial types – oligodendrocytes and astrocytes – was boosted. Our findings of the delayed neuronal maturation in post-ischemic conditions, while the NSPC differentiation was promoted towards glial cell types, provide new insights that could be applicable to stem cell therapy replacement strategies used after cerebral ischemia.

KEY WORDS: Embryonic neural stem/progenitor cell, Organotypic hippocampal slice, Maturation of neuronal excitability, Stem cell differentiation, Excitatory transmission, Cerebral ischemia

INTRODUCTION

Cerebral ischemia, a condition causing a high mortality and severe disability in patients of various ages, represents a common clinical problem worldwide, and the number of such patients progressively increases. Functional deficits produced by ischemic injury to the brain are often irreversible and can be further exacerbated some time later (i.e. following stroke) due to the massive neuronal death that can be triggered by a wide range of ischemic impairments at the cellular and subcellular levels (Baines et al., 2005; Kirino, 2000; Kopach et al., 2016; Lipton, 1999). A limited capability of the brain for neurogenesis, however, restricts the effectiveness of pharmacological therapies for anti-ischemic neuroprotection applied later than the time of the insult, thereby endorsing cell-based therapies for neuronal replacement strategies.

[1]Department of Sensory Signalling, Bogomoletz Institute of Physiology, Kyiv 01024, Ukraine. [2]Institute of Neurology, University College London, London WC1N 3BG, UK. [3]State Institute of Genetic and Regenerative Medicine, Kyiv 04114, Ukraine. [4]Kyiv Academic University, Kyiv 03142, Ukraine.

*Author for correspondence (o.kopach@ucl.ac.uk)

O.K., 0000-0002-3921-3674; V.K., 0000-0001-7636-1302; N.V., 0000-0002-2450-3134

Received 15 September 2017; Accepted 29 December 2017

Stem cells are the most promising candidate for cell-based therapy, and have gained increasing research interest over the past decades because of their broad potential for regenerative medical applications in various diseases (Meamar et al., 2013; Nedelec et al., 2013; Tornero et al., 2017; Matsa et al., 2016; Kim et al., 2002). Their therapeutic potential could be mediated by several mechanisms, namely via the acute trophic effects of stem cells on the injured tissue and their high-potent capability to differentiate into neural cells of either neuronal or glial types (Lindvall and Kokaia, 2015; Gage, 2000). In stroke-injured brain, neurons differentiated from stem cells incorporate into host circuitry (Tornero et al., 2017) and improve functional recovery (Mine et al., 2013; Tsupykov et al., 2014; Hicks et al., 2009; Oki et al., 2012). Independently of neuronal effects, neural stem/progenitor cells (NSPCs) and induced pluripotent stem cells (iPSCs) improve neurological function due to the neurotrophic effect derived from their differentiation into glial cells (predominantly, astroglia) (Emdad et al., 2012; Jiang et al., 2013). In support of the role that has emerged for astroglia in neurogenesis, stroke elicits a latent neurogenic program in astrocytes (Magnusson et al., 2014). Although cumulative evidence indicates that both neuronal and glial NSPC-derived cell types have roles in the recovery of the injured brain, the NSPC behavior (e.g. differentiation profile, electrophysiological maturation, cell activity and function) after engraftment into the post-ischemic environment remains unknown. Furthermore, although numerous studies have demonstrated the biological characteristics of the NSPC-derived neurons through combinations of immunocytochemistry and histochemistry, and cytometry and molecular biology assays, there has been much less focus on the functional properties of differentiated cells that is required to explore the appropriate neuronal physiology and integrated functional activity following engraftment (Kemp et al., 2016).

The present study shows the time courses of functional maturation and integration of the NSPC-derived neurons into the host circuits in control and post-ischemic hippocampal tissue in order to investigate how the post-ischemic environment affects the behavior of embryonic NSPCs. Our results demonstrate that there is a delayed functional maturation of the NSPC-derived neurons in an *in situ* model of cerebral ischemia, while differentiation of embryonic NSPCs towards glia is promoted.

RESULTS

Maturation of the NSPC-derived neuronal excitability *in situ*

GFP-positive uncommitted neural progenitor cells (Fig. 1A,B) were grafted onto organotypic hippocampal slices to study the maturation of their electrophysiological properties *in situ*. In total, 57 GFP-positive cells were examined in a whole-cell configuration at different time-points after engraftment (1 to 3 weeks *in situ*). For the assessment of functional maturation and the development of the appropriate electrophysiological activity, the NPSC-derived neurons were compared with endogenous CA1 pyramidal neurons.

Journal of Cell Science (2018) 131, jcs210989. doi:10.1242/jcs.210989

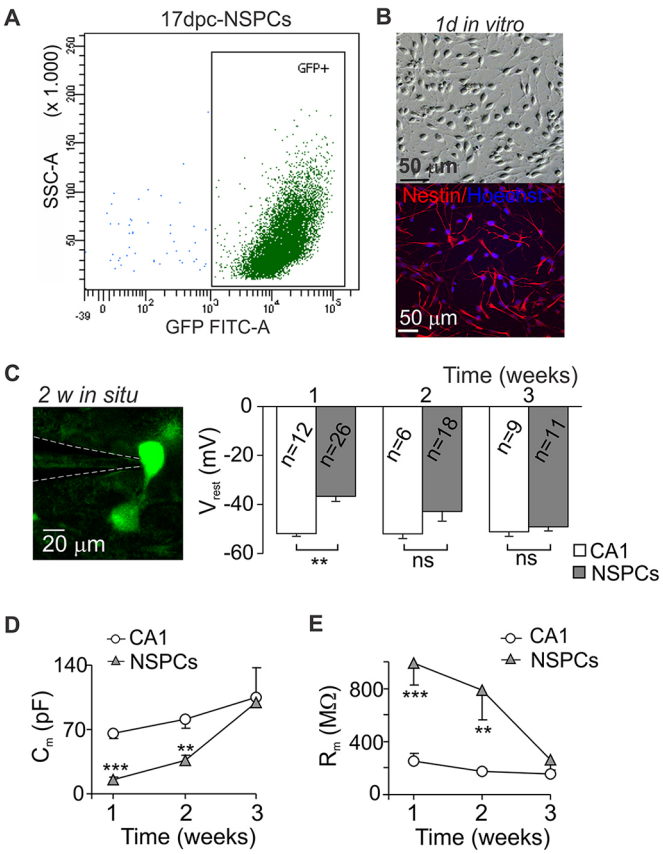

Fig. 1. Development of membrane properties in NSPCs after *in situ* engraftment. (A) FACS analysis of freshly isolated NSPCs, demonstrating a fraction of GFP-positive NSPCs (green) from viable cells. (B) Staining of the obtained cell fraction (from A) with nestin (red) and Hoechst 33342 (blue) shows the uncommitted neural progenitor cells (n=4 samples). (C) Patch-clamp of GFP-positive NSPCs (whole-cell configuration, left image) revealed the time-dependent development of the resting membrane potential (V_{rest}) in NSPCs after engraftment *in situ*. The number of cells analyzed for each group is indicated. (D,E) The time courses of changes in capacitance (C_m, D) and input resistance (R_{in}, E) of NSPCs after engraftment onto organotypic hippocampal slices. Number of NSPCs analyzed: n=26 at 1 week, n=20 at 2 weeks, n=12 at 3 weeks; host CA1 neuron, n=11 at 1 week, n=6 at 2 weeks, n=9 at 3 weeks. Data are mean±s.e.m. **P<0.01, ***P<0.001 compared to endogenous CA1 neurons (unpaired t-test); ns, non-significant.

The resting membrane potential (V_{rest}) of GFP-positive NSPCs was −36.7±4.2 mV (mean±s.e.m.; n=26) at the end of week 1 (6–7 days post-plating), −42.8±5.0 mV (n=18) at the end of week 2 (13–14 days post-plating) and −49.2±2.6 mV (n=11) at the end of week 3 (20–21 days post-plating) (Fig. 1C). When compared to endogenous CA1 neurons (1 week, −52.0±1.1 mV, n=12; 2 weeks, −52.0±2.0 mV, n=6; 3 weeks, −51.2±1.9 mV, n=9; Fig. 1C), the V_{rest} of NSPCs was less hyperpolarized at week 1 (by ∼29%; P<0.01) but did not significantly differ later on (P=0.77 and P=0.86 at 2 and 3 weeks, respectively). The NSPC capacitance gradually increased (1 week, 16.0±1.6 pF, n=26; 2 weeks, 36.6±5.5 pF, n=20; 3 weeks, 100.1±37.1 pF, n=12), reaching that in endogenous CA1 neurons by week 3 (104.4±10.8 pF for CA1 neurons, P=0.91; Fig. 1D). This indicates that there is a time-dependent increase in increase in the NSPC surface (measured for soma, including branches). In parallel, the input resistance (R_{in}) decreased, reflecting the increased conductance (an increased pool of readily available functional ion channels). In NSPCs, the R_{in} was 991.4±162.4 MΩ (n=26) and 790.3±227.4 MΩ (n=20) after 1 and 2 weeks, respectively, while it was 260.3±79.4 MΩ (n=12) after 3 weeks, thereby reaching the R_{in} in endogenous CA1 neurons (1 week, 254.8±52.4 MΩ, n=11; 2 weeks, 174.4±19.4 MΩ, n=6; 3 weeks, 158.4±21.6 MΩ, n=9; Fig. 1E).

Functional expression of both Na^+ and K^+ channels is crucial for cell excitability. To establish the time courses of the development of the Na^+- and K^+-channel-mediated conductance, we recorded the Na^+ (I_{Na}) and K^+ currents (I_K) at different time points. The voltage-clamp recordings demonstrated that both I_{Na} and I_K in NPSCs was detected as early as by week 1 (6–7 days post-grafting), with these two currents showing the voltage dependence typical of the normal I–V pattern (Fig. 2A). The total K^+-mediated conductance (consisting of fast and slow non-inactivating components) demonstrated a progressive rise of the current density at positive membrane potentials over weeks 1 to 3 (Fig. 2A*ii*) that accompanied a progressively increased density of I_{Na} (Fig. 2A*iii*). The I–V relationship also revealed Na^+ conductance at relatively low hyperpolarized potentials (−50 mV to −30 mV), which indicates functional expression of the voltage-gated Na^+ channels that activated at both subthreshold and threshold voltages (Fig. 2A*iii*).

The current-clamp recordings were next performed to assess the capability of NSPCs for generation of induced action potentials (APs). Consistent with the maturation of Na^+- and K^+-channel-mediated conductance, NSPCs showed AP generation by as early as week 1 (Fig. 2B*i*), although at a low frequency (Fig. 2B*ii*) and with AP spikes of a diminished amplitude and prolonged duration (Fig. 2C*i–iii*). The capability of NSPC-derived neurons for a high-frequency discharge developed time dependently, reaching a maximal firing rate that was comparable to that of host neurons by week 3 *in situ* (35.0±12.3 Hz versus 53.3±5.0 Hz for NSPCs and CA1 neurons, respectively; P=0.34; Fig. 2B*i*,*ii*). Other parameters of APs also developed (Fig. 2C*i–iii*).

Integration of the NSPC-derived neurons into the host circuits

Next, we examined the functional integration of the NSPC-derived neurons into the host hippocampal circuitry. To determine the time course of when neurons differentiated from NSPCs become integrated and develop the appropriate network activity, synaptic events were recorded at different time points after engraftment (1 to 3 weeks *in situ*). The voltage-clamp recordings of spontaneous excitatory postsynaptic currents (sEPSCs) at −70 mV revealed detectable events at different stages of NSPC maturation. We could detect sEPSCs as early as at 1–2 weeks post-grafting, although of a low-frequency appearance. The median frequency was 0.16 Hz (n=499 events recorded in five cells) at 1 week and 0.20 Hz (n=315 events in 8 cells) at 2 weeks (Fig. 3A*i*,*ii*). Despite a relatively low occurrence of excitatory events in NSPCs at the earlier time window, the characteristic rise kinetics of the detected currents was similar to that of endogenous CA1 neurons (Fig. 3B). Immuno-electron microscopy (EM) confirmed that NSPCs made synapses with host cells in bi-directional manner (Fig. 3C). There were numerous vesicles accumulated within the presynaptic-like structures; in some of the presynaptic structures on the host cells, vesicles were docked to the postsynaptic membrane of GFP-positive cell. After 3 weeks, the NPSC-derived neurons displayed an sEPSC frequency that was similar to that of endogenous neurons (0.95 Hz versus 1.48 Hz for NSPCs and CA1 neurons, respectively, P=0.42 the Mann–Whitney U-test; Fig. 3A*ii*). The sEPSC amplitude also increased with time after engraftment (Fig. 3D*ii*). The median amplitude was 5.37 pA and 5.71 pA at 1 and 2 weeks, respectively, but 6.71 pA at 3 weeks, a value close to that in endogenous CA1 neurons (7.45 pA, P=0.53 the Mann–Whitney U-test; Fig. 3E*i*,*ii*). The increased amplitude indicates the time-dependent functional expression of postsynaptic glutamate receptors mediating excitatory transmission.

Journal of Cell Science (2018) 131, jcs210989. doi:10.1242/jcs.210989

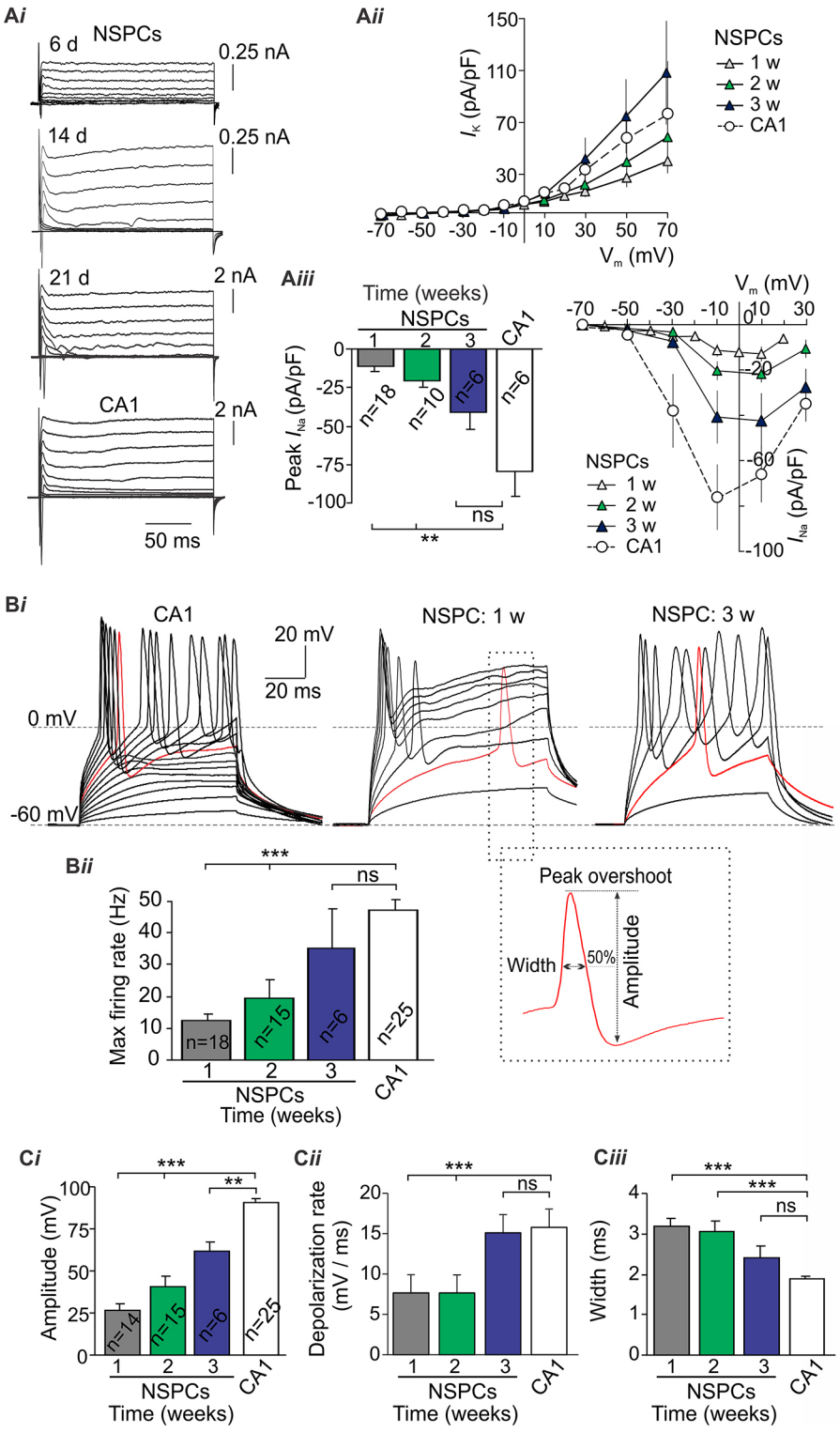

Fig. 2. The time-dependent maturation of excitability of the NSPC-derived neurons *in situ*. (A) Examples of voltage-clamp recordings from endogenous CA1 (host cell) and NSPC-derived neurons at different time-points after engraftment *in situ* (A*i*) and the average current–voltage relationship for K^+-channel-mediated conductance (I_K, A*ii*) and Na^+-channel-mediated conductance (I_{Na}, A*iii*) in host CA1 and differentiated neurons. The protocol consisted of voltage steps from −70 mV to +110 mV of 200-ms duration. The I_{Na} in endogenous CA1 neurons and NSPCs shown in A*iii* was estimated at −10 mV (the maximum over different voltages). The number of cells analyzed for each group is indicated. (B) Examples of the current-clamp recordings in endogenous CA1 (B*i* left) and the NSPC-derived neurons at 1 week (B*i* middle) and 3 weeks (B*i* right) *in situ*, and summary of the maximal firing rate in NSPCs at different time-points compared to endogenous CA1 neurons (B*ii*). Insert below, magnification of an individual AP depicting parameters of spike shaping. Red examples show the first AP evoked in the cells, where analysis of spike shaping was performed. The number of cells analyzed is indicated. (C) The time-dependent changes in individual AP spikes – amplitude (C*i*), depolarization rate (C*ii*) and the width at half-maximal amplitude (C*iii*) – in neurons differentiated from NSPCs at different time points compared to endogenous CA1 neurons. The number of host CA1 neurons: n=25; NSPCs: n=14 at 1 week, n=15 at 2 weeks, n=25 at 3 weeks for each parameters. Data are mean±s.e.m. $^{**}P<0.01$ and $^{***}P<0.001$ (unpaired t-test) compared to endogenous CA1 neurons; ns, non-significant.

Taken together, the NSPC-derived neurons integrate into the host circuitry, developing the appropriate pattern of synaptic activity (excitatory transmission) within 3 weeks *in situ*.

Delayed maturation of the NSPC-derived neuronal excitability in ischemic-impaired tissue

To examine the time-dependent maturation of electrophysiological properties of the NSPC-derived neurons in the post-ischemic environment, we exposed organotypic hippocampal slices to oxygen-glucose deprivation (OGD, 10 min duration), thereby mimicking the conditions that take place upon cerebral ischemia. Recently, we have demonstrated that this model of cerebral ischemia *in situ* triggered CA1 neuronal death within 2 weeks or less, and was accompanied by drastic functional impairments in CA1 neurons (Rybachuk et al., 2017). Therefore, the same experimental model was utilized here, followed by the NSPC therapy (Fig. 4A).

In total, 54 GFP-positive NSPCs were examined at different time points after engraftment onto the OGD-exposed tissue to compare

Journal of Cell Science (2018) 131, jcs210989. doi:10.1242/jcs.210989

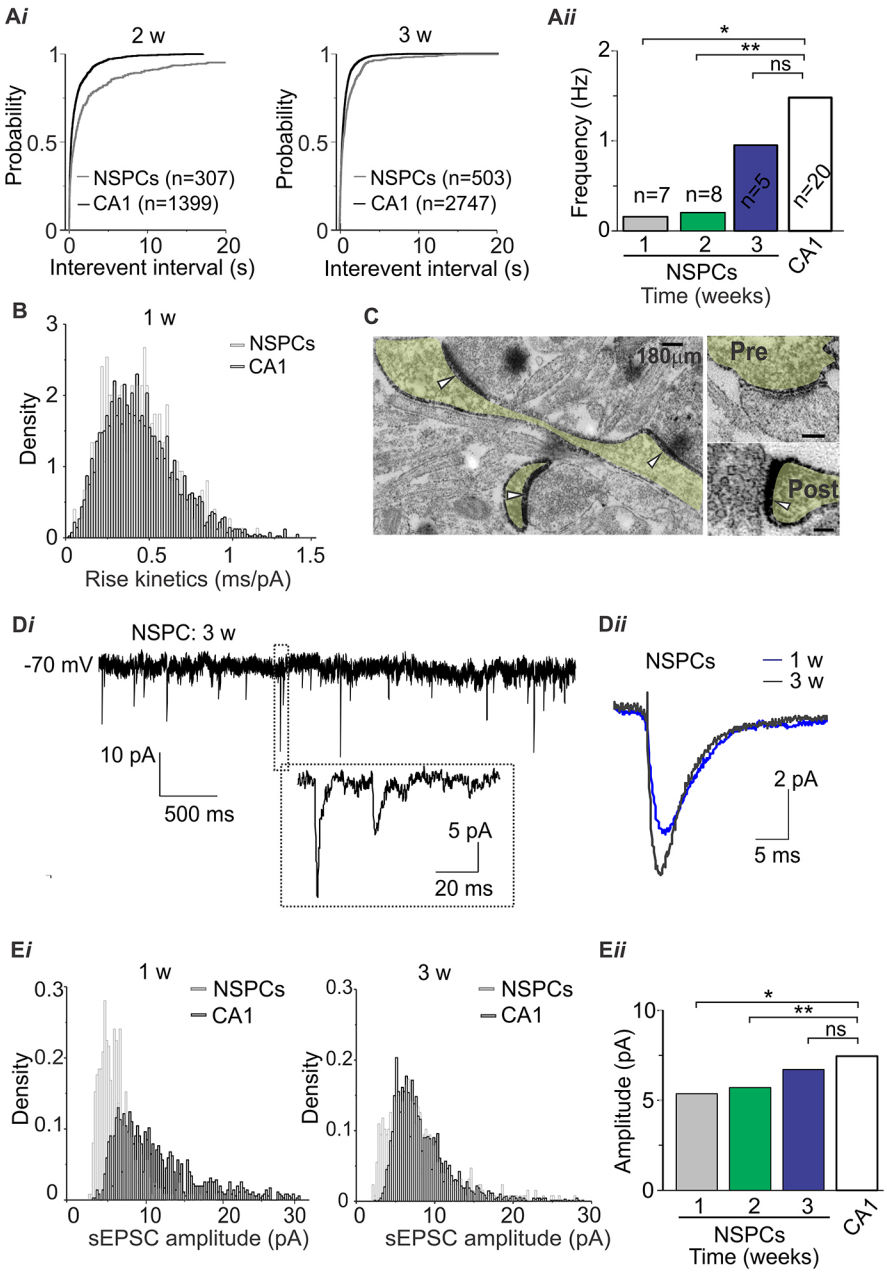

Fig. 3. The time course in which NSPC-derived neurons integrate into the host circuits. (A) Cumulative probability plots for the inter-event intervals of sEPSCs in NSPCs and endogenous CA1 neurons after different times *in situ* (A*i*) and summary of the median frequency of sEPSCs in different experimental groups (A*ii*). The sEPSC frequency is a median calculated for individual cells within the experimental group (the number of analyzed cells is indicated). Cumulative probability was analyzed for pooled events, with *n* indicating the number of events in a group. (B) Distribution profiles for the rise kinetics of sEPSCs recorded from NSPCs and endogenous CA1 neurons at the week 1. The rise-time of individual currents was normalized to the current amplitude. (C) EM images of synaptic structures between NSPCs (green overlay) and host cells in organotypic hippocampal slices. Note the numerous vesicles within presynaptic terminals and NSPCs making either pre-synaptic (pre) or postsynaptic (post) contacts. Arrows indicate the postsynaptic density on NSPCs. Scale bars for images on right: 80 nm. (D) Example of sEPSC recording from an NSPC-derived neuron at 3 weeks *in situ* (D*i*) and the average sEPSCs at 1 and 3 weeks (D*ii*). The currents are averaged from 502 events for week 1 (blue) and 341 events for the week 3 (gray). (E) Distribution profiles for the sEPSC amplitude in the NSPC-derived and CA1 neurons at different time *in situ* (E*i*) and summary of the median amplitude in different experimental groups (E*ii*). The sEPSC amplitude is median calculated for individual cells within experimental group (number of analyzed cells is the same as indicated on A*ii*). **P*<0.05, ***P*<0.01 (Mann–Whitney U-test compared to endogenous CA1 neurons); ns, non-significant.

functional properties of neurons differentiated from NSPCs in the post-ischemic environment with their counterparts in control grafts. First, we assessed the time courses of maturation of the NSPC-derived neuronal excitability in the ischemic-damaged tissue. There were no differences in the capacitance of NSPCs between control and post-ischemic conditions at week 1; however, differences appeared at later time points (week 2, 36.6±5.5 pF, n=20 in control versus 18.5±3.5 pF, n=22, P<0.01 in the OGD-exposed tissue; week 3, 100.1±37.1 pF, n=12 in control versus 60.0±17.0 pF, n=16, P=0.32 in the OGD-exposed tissue; Fig. 4B). We also found that R_{in} developed slower in NSPCs in the ischemic-damaged tissue, although the time-dependent changes did not reach a statistical difference (week 1, 991.4±162.4 MΩ, n=26 in control versus 1554.8±421.1 MΩ, n=18, in the OGD-exposed tissue, P=0.23; week 2, 790.3±227.4 MΩ, n=20 versus 1292.9±344.6 MΩ, n=22, P=0.23; week 3, 260.3±79.4 MΩ, n=12 versus 489.4±191.8 MΩ, n=16, P=0.16; Fig. 4C).

Neurons differentiated from NSPCs in the post-ischemic tissue were much less capable of generating APs than NSPC-derived neurons in control grafts. Although we detected neurons generating APs as early as 6–7 days after engraftment onto the OGD-exposed tissue, the frequency of firing was significantly lower than in control (by ∼68% at week 1, P<0.01; by ∼68% at 2 weeks, P<0.05; and by ∼49% at 3 weeks, P=0.3; Fig. 4D*ii*). The parameters of AP spike were also impaired: the amplitude was diminished (week 1, by ∼34%, P=0.12; week 2, by ∼51%, P<0.01; week 3, by ∼34%, P=0.12) and the half-amplitude width was increased in the NSPC-derived neurons in the post-ischemic tissue (Fig. 4E*i,ii*).

Moderate integration of the NSPC-derived neurons into the ischemic-impaired circuitry

Next, we examined the functional integration of NSPC-derived neurons into the ischemic-impaired circuitry. Similar to our previous findings of impaired excitatory transmission in CA1 neurons in such

Journal of Cell Science (2018) 131, jcs210989. doi:10.1242/jcs.210989

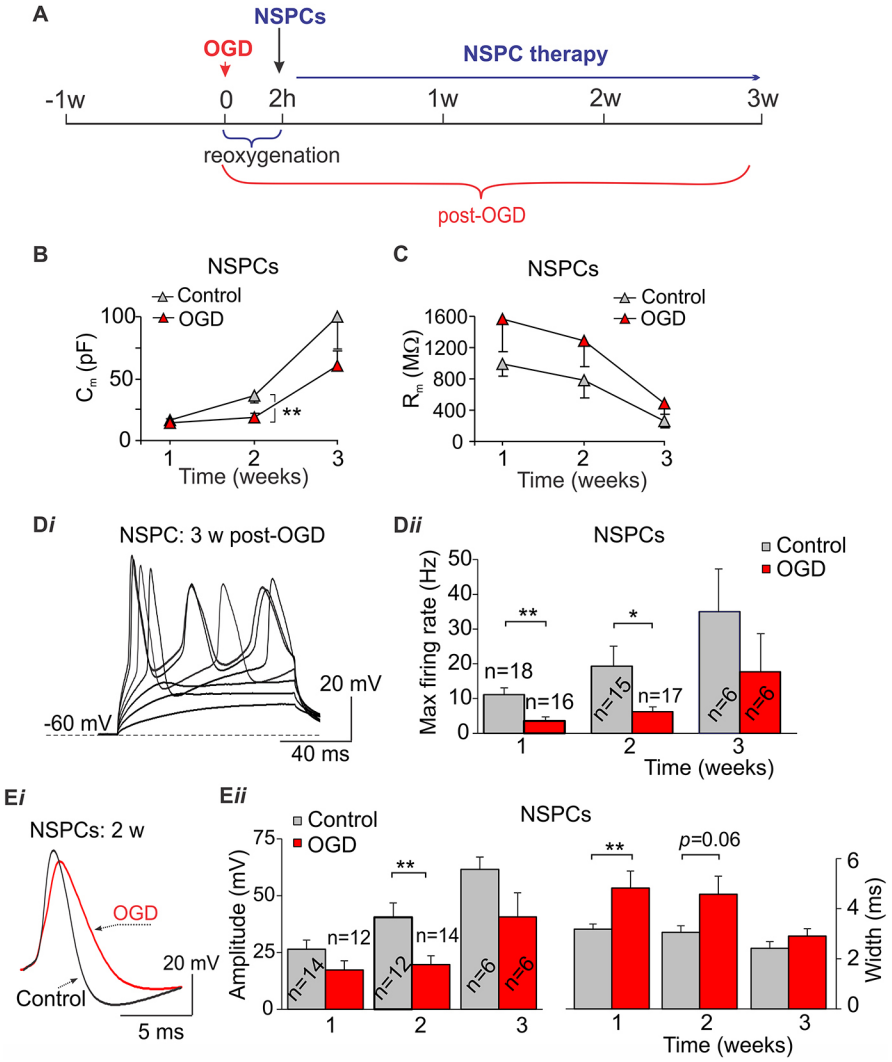

Fig. 4. Delayed maturation of neuronal excitability of NSPCs in the post-ischemic tissue. (A) Diagram of experimental modelling of cerebral ischemia *in situ* and implementing of stem cell-based therapy in hippocampal slice cultures. (B,C) The time-dependent changes in capacitance (B) and input resistance (C) of NSPCs after engraftment in control and the OGD-exposed hippocampal tissue. Number of NSPCs in control: *n*=26 at 1 week, *n*=20 at 2 weeks, *n*=12 at 3 weeks; in the post-ischemic tissue, *n*=18 at 1 week, *n*=22 at 2 weeks, *n*=16 at 3 weeks. (D) Example of AP firing by a NSPC-derived neuron at 3 weeks in the OGD-exposed tissue (D*i*), and summary of the maximal firing rate by the NSPC-derived neurons at different time points in the ischemic-impaired tissue compared to control (D*ii*). The number of cells analyzed within the groups is indicated. (E) Examples of individual AP spikes in the NSPC-derived neurons at 2 weeks in control (black) and post-ischemic tissue (red, E*i*), and summary of the time-dependent changes in AP parameters between control and post-ischemic conditions (E*ii*). The parameters of AP spike were analyzed as depicted in Fig. 2B*i*. The number of cells analyzed is indicated. Data are mean±s.e.m. **P*<0.05, ***P*<0.01 compared to the NSPC-derived neurons in control (unpaired *t*-test).

an *in situ* experimental model of cerebral ischemia (Rybachuk et al., 2017), OGD boosted the excitatory drive of CA1 neurons (enhanced sEPSC frequency) and changed postsynaptic glutamate receptors (the parameters of postsynaptic currents) in host CA1 neurons at the later period of time post OGD (1–3 weeks; data not shown). However, we did not observe any boosting of excitatory transmission in the NSPC-derived neurons in the post-ischemic tissue. No detectable sEPSCs (apart from a very few events) occurred in NSPCs at week 1 (*n*=5 cells tested); sEPSCs appeared at week 2, although at a low frequency of occurrence (four cells exhibiting detectable events out of 13 tested). After 2 weeks, the inter-event interval of sEPSCs was 2.59 s (*n*=61 events recorded in four cells) in the OGD-exposed tissue versus 0.68 s (*n*=307 events in four cells) in control tissue (*P*<0.001, Kolmogorov–Smirnov test; Fig. 5A*i*). After 3 weeks, the inter-event interval was 0.85 s (*n*=100 events recorded in four cells) versus 0.45 s (*n*=509 events in four cells; *P*<0.01 Kolmogorov–Smirnov test) in the post-OGD and control conditions, respectively (Fig. 5A*i*). The median frequency was reduced by ∼75% at 3 weeks post-OGD (*P*=0.19, Mann–Whitney *U*-test; Fig. 5A*ii*). We never observed neurons differentiated from NPSCs in the ischemic-impaired tissue developing their frequency of sEPSCs to the level of achieved by NPSCs in control tissue (or the level of host neurons). Consistent with this, the median amplitude of sEPSCs was also diminished in the NSPC-derived neurons in post-ischemic tissue (6.75 pA, *n*=6 in control, but 4.84 pA, *n*=4 in the OGD-exposed tissue at 3 weeks *in situ*; Fig. 5B*i–iii*).

Differentiation of NSPCs into glial cell types is promoted in the post-ischemic environment

So far, our results have revealed the delayed maturation of functional properties in the NSPC-derived neurons in the post-ischemic environment, with a slowed down neuronal integration into the ischemic-impaired circuitry. However, the proportion of nestin-positive cells (undifferentiated progenitors) was less in the OGD-exposed tissue compared to the proportion in control at week 1 (Fig. 6A), indicating that NSPCs differentiate in the post-ischemic environment. Our electrophysiological recordings determined that a proportion of NSPCs exhibited a V_{rest} of −70 mV (or lower) in the OGD-exposed tissue as early as 6–7 days after engraftment (Fig. 6B*i*). These cells revealed neither capability for AP generation (Fig. 6B*ii*) nor did they show voltage-dependent Na^+-currents over the time tested (1 to 3 weeks *in situ*), which matches the properties of the glial cell type. Quantitative analysis demonstrated that the proportion of NSPCs exhibiting V_{rest} ≤−70 mV was higher in the post-ischemic tissue than in the control at each time point tested (Fig. 6C). Consistent with this, the proportion of NSPCs not capable of firing was also higher (control, 25% to 40% at 1 and 3 weeks, respectively; post-OGD, 50% to

Journal of Cell Science (2018) 131, jcs210989. doi:10.1242/jcs.210989

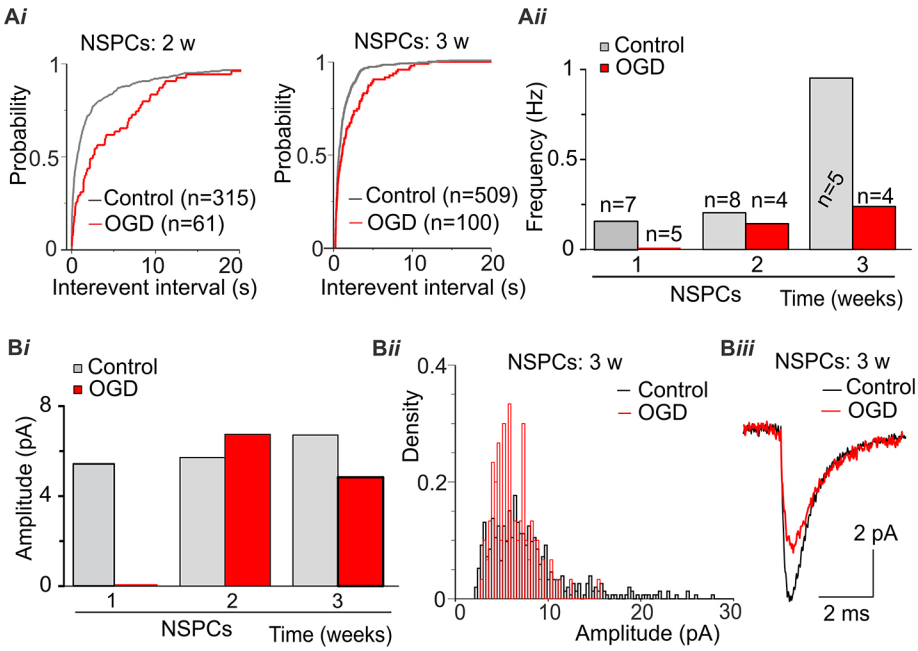

Fig. 5. Decelerated integration of the NSPC-derived neurons into the ischemic-impaired hippocampal circuits. (A) Cumulative probability plots for the inter-event intervals of sEPSCs in the NSPC-derived neurons at different time-points in control and post-ischemic tissue (A*i*) and summary of the frequency of sEPSCs in different groups of differentiated neurons (A*ii*). The sEPSC frequency is the median calculated for individual NSPCs in experimental groups (the number of cells analyzed is indicated). Cumulative probability shows pooled events, with *n* indicating the number of events in a group. (B) Summary of the sEPSC amplitude in the NSPC-derived neurons at different times after engraftment in control and post-ischemic tissue (B*i*), and distribution profiles for the sEPSC amplitude at 3 weeks for each condition (B*ii*). The overlay of the average sEPSCs at 3 weeks *in situ* (B*iii*) demonstrates the reduced current amplitude in post-ischemic tissue compared to control. The currents are average from 341 events in control (black) and 80 events post OGD (red).

80%, respectively; Fig. 6D). Taken together, this demonstrates that differentiation of NSPCs is promoted towards glial type in the post-ischemic environment.

The pool of identified NSPC-derived glial cells was not homogenous according to electrophysiological properties of the cells, as it varied in both R_{in} (from few MΩ to a few GΩ) and capacitance (Fig. 6E). Immunohistology further confirmed the NSPC differentiation into different glial cell types – oligodendrocytes and astrocytes (Fig. 6F).

DISCUSSION

A broad therapeutic potential of stem cells has led to increasing interest in cell-based therapies for cell replacement strategies in neuronal cell loss after stroke, brain injury or in neurodegenerative diseases (Lindvall and Kokaia, 2015; Meamar et al., 2013; Pluchino et al., 2003; Kim et al., 2002). Such strategies include either transplantation of cells that are already differentiated into the injured tissue (Tornero et al., 2017; Kim et al., 2002) or engraftment of stem cells into a host tissue for subsequent differentiation and maturation (de la Rosa-Prieto et al., 2017; Tsupykov et al., 2014; Darsalia et al., 2011; Mine et al., 2013). The latter approach is considered as one promoting multipotent differentiation of neural precursors in an environment of endogenous cells in order to provide 'self-repair' of injured tissue (Gage, 2000), although such a concept remains debatable. In this study, we aimed to determine the time course of maturation of the functional properties of neurons derived from embryonic NSPCs and their integration into the host circuits. We document development of the appropriate neuronal activity (comparable to host endogenous CA1 neurons) that takes 3 weeks or less after engraftment of embryonic NSPCs in hippocampal tissue *in situ*. We further demonstrate the role of the host environment in regulating the maturation of the NSPC-derived neurons and the differentiation profile by comparing functional properties of the NSPC-derived cells between control and post-ischemic conditions at different time windows.

Improving neurogenesis and accelerating functional maturation of the NSPC-derived cells have been long-desired tasks, being realized through the utilization of purposely designed enhanced media consisting of various transcriptional factors or cocktail composites. However, the survival rate of differentiated cells after transplantation remains relatively low and neurons differentiated from NSPCs or iPSCs in *in vitro* conditions often exhibit functional deficits. With this idea, we aimed to examine the time course of functional maturation of NSPC-derived neurons in the endogenous (physiological) environment where both tissue architecture and signaling pathways remained preserved. Since we have recently established that mouse organotypic hippocampal slices can be suitable for long-term maintenance (at least 4–5 weeks), with no functional deficit in CA1 neurons over this time window (Rybachuk et al., 2017), here, we focused on the functional (electrophysiological) properties of neurons derived from embryonic NSPCs. These NSPCs were grafted into hippocampal tissue in basic artificial medium (no enriched composites) in order to trace the maturation of NSPCs in a host (endogenous) environment. Neuronal maturation was assessed with regard to developing of passive membrane properties, cell excitability and network activity (integration into the host circuits). We observed progressively improving parameters of V_{rest}, capacitance (increasing cell surface), and R_{in} (readout of conductance, i.e. the readily available pool of functional ion channels) over the week 1 to 3 *in situ*, together demonstrating the time-dependent development of functional properties of the cells. Consistently, NSPCs gradually developed their neuronal excitability, including Na^+- and K^+-mediated conductance and the capability for generating induced APs. Remarkably, we observed cells capable of firing shortly after engraftment (6–7 days *in situ*), although these cells did not maintain a high-frequency discharge within the earlier time frames examined (1–2 weeks). These results are similar to the properties of human NSPCs in rat hippocampal slices reported for such a time frame (Morgan et al., 2012). Consistent with the maturation of neuronal excitability, we detected synaptic activity in the NSPC-derived neurons as early as by week 1 post-grafting, although detected sEPCSs, which are indicative of functional synapses between differentiated NSPCs and host cells, occurred at very low frequency. EM confirmed synaptic structures, showing that there were numerous vesicles within presynaptic terminals at such a time frame. Interestingly, the same frequency of sEPSCs was detected in human NSPCs at 4 DIV *in situ* (Morgan et al., 2012). The parameters of

Journal of Cell Science (2018) 131, jcs210989. doi:10.1242/jcs.210989

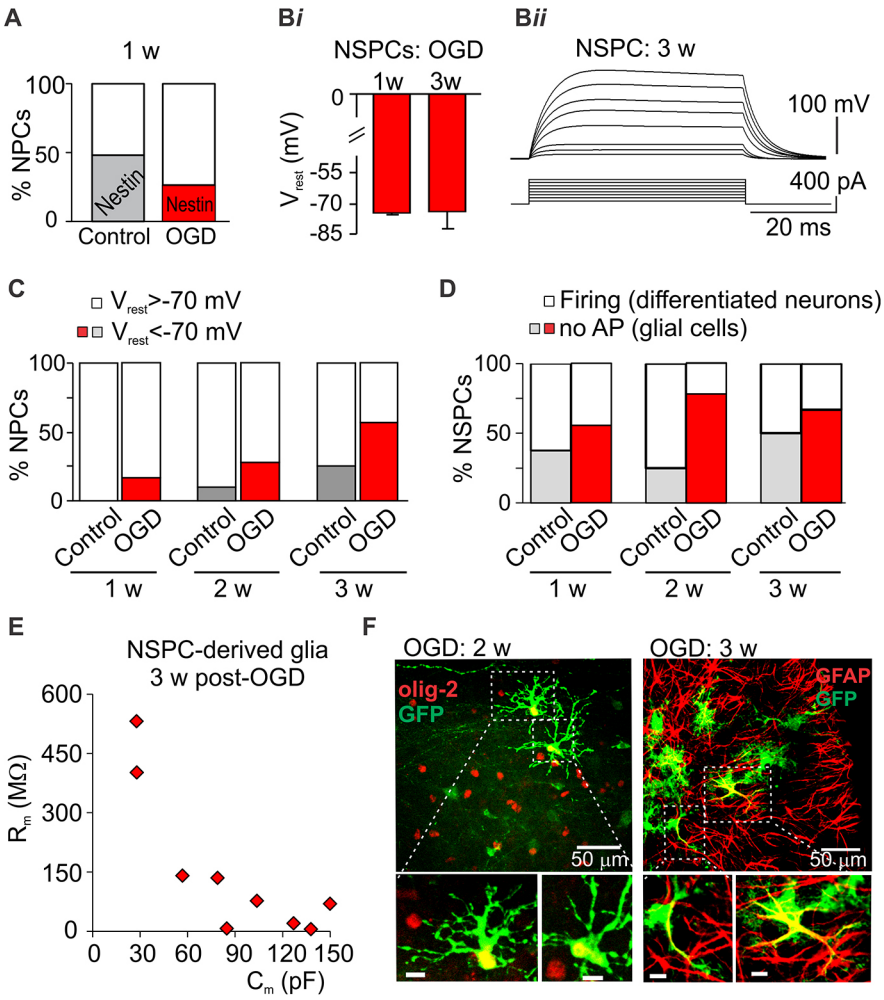

Fig. 6. Promoted NSPC differentiation towards glial cell type in the post-ischemic environment. (A) Proportion of nestin-positive NSPCs at week 1 in control and the OGD-exposed tissue. (B) Summary of the resting membrane potential (V_{rest}) of NSPCs in the OGD-exposed hippocampal slices (B*i*) and example of the current-clamp recordings from NSPCs at 3 weeks showing no AP firing (B*ii*). Number of NSPCs: *n*=5 at 1 week, *n*=9 at 3 weeks. (C) The time-dependent changes in relative proportions of NSPCs displaying V_{rest}≤−70 mV to NSPCs with V_{rest}≥−70 mV in control and post-ischemic conditions. Number of total cells analyzed for control group: *n*=26 at 1 week, *n*=20 at 2 weeks and *n*=12 at 3 weeks; for the OGD-exposed tissue, *n*=18 at 1 week, *n*=22 at 2 weeks and *n*=16 at 3 weeks. (D) The time-dependent changes in relative proportions of NSPCs displaying firing and those failed to fire in control and post-ischemic conditions. Number of total cells analyzed for control group: *n*=24 at 1 week, *n*=16 at 2 weeks and *n*=12 at 3 weeks; in the OGD-exposed tissue, *n*=18 at 1 week, *n*=18 at 2 weeks and *n*=15 at 3 weeks. (E) Scatter-plot of the R_{in} values plotted against capacitance (C_m) of the NSPC-derived glial cells at 3 weeks in the OGD-exposed tissue. The NSPC-derived glial cells were identified as those displaying V_{rest} of −70 mV (or lower) and not firing. (F) Example images of positive staining of NSPCs for Olig-2, a marker for oligodendrocytes, and the astrocytic marker GFAP in the CA1 area in the OGD-exposed tissue. Scale bars for images on the bottom: 10 µm.

postsynaptic currents reached those in endogenous CA1 neurons after 3 weeks *in situ* (both frequency and amplitude), thus arguing for proper integration of differentiated neurons into the host circuits and maturation of the postsynaptic receptors. Taken together, our data demonstrate that maturation of the NSPC-derived neurons takes 3 weeks or less in a host tissue, pointing at the accelerated maturation *in situ* when compared with the similar functional parameters of NSPCs within such time frame in *in vitro* conditions (Morgan et al., 2012; Lam et al., 2017). This indicates a regulatory role of physiological environment in stem cell maturation. In support of the accelerated neuronal maturation within a host environment, iPSC-derived neurons developed their functional properties (V_{rest}, Na^+- and K^+-currents) within a similar time window (3 weeks) *in vitro* in a medium enriched with transcriptional factors (Colasante et al., 2015). On the other hand, the physiological environment of organotypic tissue cultures might be compromised by a lack of blood flow and morphological modifications with increasing time of tissue maintenance. It remains unclear whether conditions *in vivo* accelerate the maturation of neural precursor cells since the functional properties of differentiated neurons (firing pattern or network activity) are typically studied a few months following their transplantation into the brain (Zhou et al., 2015; Avaliani et al., 2014; Tornero et al., 2017; Oki et al., 2012).

We recently described in detail the ischemic impairments, both morphological and functional, in organotypic hippocampal slices at the later time window (1–3 weeks) following OGD (Rybachuk et al., 2017). Therefore, here, we focused on the maturation of NSPC-derived neurons *in situ* as a possible NSPC therapy for cell replacement strategies after cerebral ischemia. However, the NSPC-derived neurons exhibited slower maturation of their functional properties in the OGD-exposed tissue than in control. All electrophysiological parameters (capacitance and resistance, firing discharge and shaping of APs) matured slower in the OGD-exposed tissue at each time point tested (1 to 3 weeks). The integration of NSPCs into the impaired host circuits was also delayed compared with that in control – we rarely detected synaptic events in the NSPC-derived neurons at 1–2 weeks, and the sEPSC parameters remained lower even following 3 weeks *in situ*. Such functional deficits very likely relate to severe post-ischemic impairments in hippocampal tissue due to glutamate-induced excitotoxicity and overwhelmed depolarization of endogenous neurons (Dzhala et al., 2001; Fujiwara et al., 1987), which persist for 2–3 weeks after OGD (Rybachuk et al., 2017). In contrast to the delayed neuronal maturation, NSPC differentiation to a glial cell type was boosted in the post-ischemic environment. We identified this by showing that an increased proportion of NSPCs (1) exhibited a V_{rest} lower than −70 mV as early as 5–7 days after engraftment [for comparison, iPSC-derived neurons develop a V_{rest} from −50 mV to −58 mV after 5 months following transplantation in stroke-damaged brain (Oki et al., 2012)] and those cells (2) displayed no firing (or Na^+-channel-mediated currents) over the time tested (1 to 3 weeks). Both electrophysiological properties characterize the glial cell type. According to the various membrane properties recorded for NSPC-derived glial cells, immunostaining further confirmed the NSPC differentiation into at least two different glial cell types –

oligodendrocytes and astrocytes. The versatile differentiation of NSPCs into, for example, neurons (Kelly et al., 2004; Tornero et al., 2017), astrocytes (Emdad et al., 2012; Jiang et al., 2013), oligodendrocytes (Pluchino et al., 2003) and even endovascular cells (Wurmser et al., 2004) has been firmly shown previously; therefore, it is not surprising here, but the distinct differentiation profile between control and post-ischemic conditions have not been shown to date. The changes in migration and outgrowth of human iPSCs after transplantation in stroke-injured brain have been recently reported, but cell proliferation and differentiation were not altered (de la Rosa-Prieto et al., 2017). By using an electrophysiological approach for functional characterization of embryonic NSPCs, here, we demonstrate enhanced NSPC differentiation towards the glial cell type in the ischemic-impaired tissue, which was accompanied with delayed functional maturation (electrophysiological properties) of NSPC-derived neurons. These results indicate the regulatory role of host environment for stem cell activity and also suggest that glia have the role in determining post-ischemic conditions. Although the mechanisms through which glia impact on ischemic impairments remain to be defined, at first glance, the NSPC-derived glial cells, identified here as oligodendrocytes and astrocytes, provide a profound neurotrophic effect on the impaired tissue. Oligodendrocytes differentiated from NSPCs essentially contributed to the axon re-myelination and the NSPC-derived astrocytes supported axonal regeneration and neuronal survival by secreting numbers of neurotrophic and growth factors (Davies et al., 2006; Shetty et al., 2005). Hypothetically, a latent neurogenic program could be elicited in astrocytes upon ischemic conditions (Magnusson et al., 2014) to promote neurogenesis, enhance proliferation and differentiation of precursor cells, control cell migration and axon guidance (Lu and Kipnis, 2010; Staquicini et al., 2009).

Summarizing, our results show that post-ischemic environment alters functional maturation of the NSPC-derived neurons and the identity of pool of NSPCs engrafted in the ischemic-damaged hippocampal tissue *in situ*. Our findings showing the role of host environment in differentiation and maturation of NSPCs provide new insights that could be useful when considering stem cell-based therapy for neuronal replacement after cerebral ischemia and, thereby, the potential of NSPC-derived cell types as an anti-ischemic treatment.

MATERIALS AND METHODS

Organotypic hippocampal slice cultures

Animals were used in accordance with the protocols approved by the Animal Care and Use Committee at Bogomoletz Institute of Physiology (Kyiv, Ukraine) and the European Commission Directive (86/609/EEC). Organotypic hippocampal slice cultures were prepared from 8–9-day-old FVB mice, as described in detail recently (Rybachuk et al., 2017). Briefly, after the hippocampi were dissected out, transverse slices (350-µm thick) were cut and placed on 0.4-µm membrane inserts (Sigma, Millicell®CM, Germany). Slices were maintained in culture medium containing 50% MEM, 25% HBSS, 25% horse serum, 2.5 mM Tris, 2 mM $NaHCO_3$, 12.5 mM HEPES, 15 mM glucose and 1% penicillin-streptomycin at 37°C (5% CO_2). Medium was replaced on the day 2 after plating and then twice a week.

Isolation of NSPCs and fraction analysis

NSPCs were isolated from the hippocampi of 16–17 days post coitum (dpc) embryos from FVB-Cg-Tg(GFPU) 5Nagy/J transgenic mice expressing GFP (Tsupykov et al., 2014) by means of centrifugation (450 ***g***, 10 min) of a cell suspension in 22% Percoll (GE Healthcare BioScience, Sweden). Flow cytometry was performed in the enriched cell fraction (5×10^5 cells in 100 µl phosphate-buffered saline, PBS) using the BD FACS Aria cell sorter with BD FACSDiva™ 6.1.2 software (BD Biosciences). The percentage of viable cells was assessed by using 7-aminoactinomycin D (7-AAD, BD Pharmingen) (2.5 µg/ml, 10 min at 4°C). Unstained samples were used as a control. The average numbers of GFP-positive and 7-AAD-negative cells from at least 20×10^3 cells per sample were counted. FACS analysis demonstrated that a freshly isolated suspension of NSPCs consisted of 85–90% viable cells, with ∼95–99.6% GFP positive (Fig. 1A).

NSPCs were plated on Matrigel-coated coverslips (BD Biosciences) in a four-well plate (5×10^4 cells/well) in neurobasal medium (Gibco), supplemented with 20 ng/ml FGF-2 (Sigma), B27 (2%, Invitrogen), 1 mM sodium pyruvate (Sigma), 1 mM N-acetyl-L-cysteine (Sigma), 1% L-glutamine (HyClone) and 1% penicillin-streptomycin (Invitrogen) at 37°C (5% CO_2). At 1–2 days *in vitro*, cells were fixed with 4% paraformaldehyde (PFA, 30 min), washed out with 0.1 M phosphate buffer (PB), and blocked with 0.3% Triton X-100 and 0.5% BSA. The primary antibodies used were monoclonal mouse anti-nestin, a marker of uncommitted neural progenitor cells (1:500; MAB353, Millipore). The secondary antibodies were donkey anti-mouse-IgG conjugated to Alexa Fluor 555 (A-31570, Invitrogen). The nuclei were labeled with Hoechst 33342 (1:5000; H3570, Invitrogen).

OGD and engraftment of NSPCs *in situ*

Freshly isolated NSPCs were grafted onto the organotypic slices (7 days post-plating) at a density of 0.25×10^5 cells *per* slice. For the OGD-exposed tissue, the organotypic hippocampal slice cultures were exposed to oxygen-glucose deprivation (OGD, 10-min duration), as we described recently (Rybachuk et al., 2017). Briefly, slice cultures (7 days post-plating) were placed into medium containing 15 mM sucrose (instead of 15 mM glucose), and equilibrated with 95% N_2 and 5% CO_2 for 10 min. After termination of OGD, the tissue was returned into culture medium and maintained until used. NSPCs were grafted 2 h post-OGD (Fig. 4A). At 1 day after engraftment, medium was replaced to wash out NSPCs not attached to a host tissue. Quantitative analysis demonstrated that there were a similar number of NSPCs over the time of the experiment (1–2 weeks after engraftment) for the control and the OGD-exposed slices (data not shown), consistent with other reports (Darsalia et al., 2011; Sakata et al., 2012; Hicks et al., 2009; de la Rosa-Prieto et al., 2017).

Immunohistochemistry

Organotypic hippocampal slice cultures were fixed with 4% PFA overnight, washed with 0.1 M PB, and blocked in 0.1 M PB containing 0.3% Triton X-100 and 0.5% bovine serum albumin (BSA). The following primary antibodies were used: monoclonal mouse anti-neuronal nuclei (NeuN, 1:1000; MAB377, Chemicon), polyclonal chicken anti-glial fibrillary acidic protein (GFAP, 1:1500; ab4674, Abcam), polyclonal rabbit anti-olig-2 (1:1000; AB9610, Chemicon) and polyclonal goat anti-GFP antibodies (1:700; 100-1770 Novus Biologicals, USA). Secondary antibodies were donkey anti-goat-IgG conjugated to Alexa Fluor 488 (1:1000; A-11055, Invitrogen), donkey anti-mouse-IgG conjugated to Alexa Fluor 555 (A-31570, Invitrogen, USA), goat anti-chicken-IgG conjugated to Alexa Fluor 647 (1:1000; A-21449, Invitrogen) or donkey anti-rabbit IgG conjugated to Alexa Fluor 647 (1:1000; A-31573, Invitrogen, USA). Slices were mounted on glass slides with DakoCytomation fluorescent mounting medium (DacoCytomation). Confocal images were taken using a FV1000-BX61WI laser scanning microscope (Olympus, Tokyo, Japan). Analysis of images was performed using ImageJ (NIH, USA).

Electrophysiology

The whole-cell recordings were made from endogenous CA1 neurons (host cells) and GFP-positive NSPCs in organotypic slice cultures at different time-points of tissue maintenance/post-grafting of NSPCs. Recordings were made in artificial cerebrospinal fluid (ACSF) containing (in mM): 124 NaCl, 1.6 KCl, 24 $NaHCO_3$, 1.2 KH_2PO_4, 2.5 $CaCl_2$, 1.5 $MgCl_2$, 2 ascorbic acid, and 10 glucose (95% O_2 and 5% CO_2, pH 7.4). Intracellular solution was (in mM): 133 K-gluconate, 5 NaCl, 0.5 $MgCl_2$, 10 HEPES-Na, 2 MgATP, 0.1 GTP-Na and 0.5 EGTA (pH 7.2, osmolarity 290 mOsM). Patching pipettes had a resistance of 3–5 MΩ. Cells were recorded in current and voltage-clamp modes using a MultiClamp 700B amplifier (Axon Instruments, Molecular Devices, CA); cells displaying a leak current >100 pA were discarded. GFP-positive NSPCs were fluorescently identified by using an

Olympus BX50WI microscope (Olympus, Japan), equipped with a 60×, NA 0.9 water-immersion objective and DIC optics, and a PolyChrome IV monochromator (Till Photonics, Germany) with a 12-bit cooled CCD camera (Sensicam, PCO, Germany) operated with Imaging Workbench software (INDEC System).

NSPCs were studied for (1) passive membrane properties, including the resting membrane potential (V_{rest}), capacitance (C_m) and input resistance (R_{in}), and for (2) neuronal excitability and (3) functional integration into the host hippocampal circuits (synaptic activity). Capacitance measurements were performed by using a common protocol of integrating the transient capacitive current during the voltage-clamp steps with pClamp software (Molecular Devices, CA); the parameter was measured for soma, including proximal branches, rather than over the entire architecture of neuronal processes (Golowasch et al., 2009). Neuronal firing was elicited with a series of depolarizing currents of 50- to 100-ms duration applied with increased stimulus intensity (30–60 pA increment). We analyzed the frequency of firing and the parameters of AP spike for its amplitude, peak overshoot, depolarization rate and the spike width at half-maximal amplitude. Only the first AP spike generated by a cell was used for the analysis. For the current-voltage relationship (*I–V* curves) for the Na^+-channel- and K^+-channel-mediated currents, voltage steps of 200-ms duration were applied from −70 mV with an increment 10 to 20 mV. Functional integration of the NSPC-derived neurons into hippocampal circuits was examined by recording the sEPSCs at −70 mV.

Clampfit 10.3 software (Molecular Devices, CA) and Origin Pro (Origin Lab) were used for analysis. The Mini Analysis Program (Synaptosoft, Decatur, GA) was used for off-line detection of sEPSCs, as we have described in detail elsewhere (Kopach et al., 2015; Kopach et al., 2017). Excitatory currents were distinguished from baseline noise by setting the appropriate parameters for each individual cell and manually eliminating false-positive events. The currents were analyzed for the frequency of occurrence, and their amplitude and kinetics calculated within the time frame of 0% to 100% of current rise time normalized to the amplitude.

Immuno-electron microscopy

For visualization of synaptic structures between host cells and grafted NPSCs, immuno-electron microscopy was used as described in detail previously (Tsupykov et al., 2014). Briefly, slices were fixed with 4% PFA and 0.25% glutaraldehyde in 0.1 M PB for 1 h at room temperature. After fixation, slices were washed with 0.1 M PB, treated with 0.3% H_2O_2 for inactivation of endogenous peroxidases (15 min) and permeabilized with 0.1% Triton X-100 in blocking solution (5% BSA and 5% normal goat serum) for 30 min at 4°C. Afterwards, slices were incubated with polyclonal rabbit anti-GFP antibodies (1:500; A-11122, Molecular Probes, Eugene, OR) for 48 h at 4°C. For negative control primary antibodies were omitted and slices were incubated in blocking solution. Secondary antibodies were horseradish peroxidase (HRP)-conjugated goat anti-rabbit-IgG (H+L) (1:200; 34506SB, MoBiTec, Germany) incubated for 24 h at 4°C. Subsequently, the standard diaminobenzidine (DAB) reaction was performed, slices were post-fixed in osmium tetroxide, then dehydrated in an increasing ethanol series, pre-embedded with propylene oxide, and flat-embedded in epoxy resin (agar 100 resin, araldite CY 212, DDSA, DMP-30; Plano, Wetzlar, Germany). For identifying the GFP (DAB-labeled) cells semi-thin sections were stained with Methylene Blue. Finally, ultra-thin sections were stained with uranyl acetate and lead citrate and examined in an electron microscope (JEOL100-CX; JEOL, Tokyo, Japan) at 80 kV.

Statistical analysis

All data are presented as mean±s.e.m. with *n* referring to the number of cells analyzed. A Student's two-tailed *t*-test was used to determine statistical differences between different experimental groups. The data sets for the recorded sEPSCs were probed for normality with the Shapiro–Wilk test. Mostly, the data sets were not normally distributed, therefore, they were compared using a nonparametric Mann–Whitney *U*-test; those results are presented as medians. The Kolmogorov–Smirnov two-sample test was used to compare the distributions in parameters between groups. A *P* value less than 0.05 was considered as statistically significant for either test.

Acknowledgements

The authors thank Dr Oleg Tsupykov and Mrs Ekaterina Smozhanik for the assistance in immuno-electron microscopy.

Competing interests

The authors declare no competing or financial interests.

Author contributions

Conceptualization: O.K., T.P.; Methodology: O.K., O.R., T.P.; Validation: O.K.; Formal analysis: O.K., O.R., V. Krotov, V. Kyryk; Investigation: O.K., O.R.; Resources: N.V., T.P.; Data curation: O.K., T.P.; Writing - original draft: O.K., T.P.; Writing - review & editing: O.K.; Visualization: O.K., O.R., V. Kyryk; Supervision: T.P.; Project administration: T.P.; Funding acquisition: N.V., T.P.

Funding

This work was supported by the State Fund for Fundamental Research of Ukraine (F46.2/001 to T.P. and N.V.) and the National Academy of Sciences of Ukraine (Biotechnology and Functional Genomics grant CPV-15/16/17/18 to N.V.).

References

Avaliani, N., Sørensen, A. T., Ledri, M., Bengzon, J., Koch, P., Brüstle, O., Deisseroth, K., Andersson, M. and Kokaia, M. (2014). Optogenetics reveal delayed afferent synaptogenesis on grafted human-induced pluripotent stem cell-derived neural progenitors. *Stem Cells* **32**, 3088-3098.

Baines, C. P., Kaiser, R. A., Purcell, N. H., Blair, N. S., Osinska, H., Hambleton, M. A., Brunskill, E. W., Sayen, M. R., Gottlieb, R. A., Dorn, G. W. et al. (2005). Loss of cyclophilin D reveals a critical role for mitochondrial permeability transition in cell death. *Nature* **434**, 658-662.

Colasante, G., Lignani, G., Rubio, A., Medrihan, L., Yekhlef, L., Sessa, A., Massimino, L., Giannelli, S. G., Sacchetti, S., Caiazzo, M. et al. (2015). Rapid conversion of fibroblasts into functional forebrain GABAergic interneurons by direct genetic reprogramming. *Cell Stem Cell* **17**, 719-734.

Darsalia, V., Allison, S. J., Cusulin, C., Monni, E., Kuzdas, D., Kallur, T., Lindvall, O. and Kokaia, Z. (2011). Cell number and timing of transplantation determine survival of human neural stem cell grafts in stroke-damaged rat brain. *J. Cereb. Blood Flow Metab.* **31**, 235-242.

Davies, J. E., Huang, C., Proschel, C., Noble, M., Mayer-Proschel, M. and Davies, S. J. A. (2006). Astrocytes derived from glial-restricted precursors promote spinal cord repair. *J. Biol.* **5**, 7.

de La Rosa-Prieto, C., Laterza, C., Gonzalez-Ramos, A., Wattananit, S., Ge, R., Lindvall, O. and Tornero, D. (2017). Stroke alters behavior of human skin-derived neural progenitors after transplantation adjacent to neurogenic area in rat brain. *Stem Cell Res. Ther.* **8**, 59.

Dzhala, V., Khalilov, I., Ben-Ari, Y. and Khazipov, R. (2001). Neuronal mechanisms of the anoxia-induced network oscillations in the rat hippocampus in vitro. *J. Physiol.* **536**, 521-531.

Emdad, L., D'souza, S. L., Kothari, H. P., Qadeer, Z. A. and Germano, I. M. (2012). Efficient differentiation of human embryonic and induced pluripotent stem cells into functional astrocytes. *Stem Cells Dev.* **21**, 404-410.

Fujiwara, N., Higashi, H., Shimoji, K. and Yoshimura, M. (1987). Effects of hypoxia on rat hippocampal neurones in vitro. *J. Physiol.* **384**, 131-151.

Gage, F. H. (2000). Mammalian neural stem cells. *Science* **287**, 1433-1438.

Golowasch, J., Thomas, G., Taylor, A. L., Patel, A., Pineda, A., Khalil, C. and Nadim, F. (2009). Membrane capacitance measurements revisited: dependence of capacitance value on measurement method in nonisopotential neurons. *J. Neurophysiol.* **102**, 2161-2175.

Hicks, A. U., Lappalainen, R. S., Narkilahti, S., Suuronen, R., Corbett, D., Sivenius, J., Hovatta, O. and Jolkkonen, J. (2009). Transplantation of human embryonic stem cell-derived neural precursor cells and enriched environment after cortical stroke in rats: cell survival and functional recovery. *Eur. J. Neurosci.* **29**, 562-574.

Jiang, P., Chen, C., Wang, R., Chechneva, O. V., Chung, S. H., Rao, M. S., Pleasure, D. E., Liu, Y., Zhang, Q. and Deng, W. (2013). hESC-derived Olig2+ progenitors generate a subtype of astroglia with protective effects against ischaemic brain injury. *Nat. Commun.* **4**, 2196.

Kelly, S., Bliss, T. M., Shah, A. K., Sun, G. H., Ma, M., Foo, W. C., Masel, J., Yenari, M. A., Weissman, I. L., Uchida, N. et al. (2004). Transplanted human fetal neural stem cells survive, migrate, and differentiate in ischemic rat cerebral cortex. *Proc. Natl. Acad. Sci. USA* **101**, 11839-11844.

Kemp, P. J., Rushton, D. J., Yarova, P. L., Schnell, C., Geater, C., Hancock, J. M., Wieland, A., Hughes, A., Badder, L., Cope, E. et al. (2016). Improving and accelerating the differentiation and functional maturation of human stem cell-derived neurons: role of extracellular calcium and GABA. *J. Physiol.* **594**, 6583-6594.

Kim, J.-H., Auerbach, J. M., Rodríguez-Gómez, J. A., Velasco, I., Gavin, D., Lumelsky, N., Lee, S.-H., Nguyen, J., Sánchez-Pernaute, R., Bankiewicz, K. et al. (2002). Dopamine neurons derived from embryonic stem cells function in an animal model of Parkinson's disease. *Nature* **418**, 50-56.

Kirino, T. (2000). Delayed neuronal death. *Neuropathology* **20** Suppl, S95-S97.
Kopach, O., Krotov, V., Belan, P. and Voitenko, N. (2015). Inflammatory-induced changes in synaptic drive and postsynaptic AMPARs in lamina II dorsal horn neurons are cell-type specific. *Pain* **156**, 428-438.
Kopach, O., Maistrenko, A., Lushnikova, I., Belan, P., Skibo, G. and Voitenko, N. (2016). HIF-1alpha-mediated upregulation of SERCA2b: the endogenous mechanism for alleviating the ischemia-induced intracellular Ca(2+) store dysfunction in CA1 and CA3 hippocampal neurons. *Cell Calcium* **59**, 251-261.
Kopach, O., Medvediev, V., Krotov, V., Borisyuk, A., Tsymbaliuk, V. and Voitenko, N. (2017). Opposite, bidirectional shifts in excitation and inhibition in specific types of dorsal horn interneurons are associated with spasticity and pain post-SCI. *Sci. Rep.* **7**, 5884.
Lam, R. S., Topfer, F. M., Wood, P. G., Busskamp, V. and Bamberg, E. (2017). Functional maturation of human stem cell-derived neurons in long-term cultures. *PLoS One* **12**, e0169506.
Lindvall, O. and Kokaia, Z. (2015). Neurogenesis following stroke affecting the adult brain. *Cold Spring Harb. Perspect. Biol.* **7**, a019034.
Lipton, P. (1999). Ischemic cell death in brain neurons. *Physiol. Rev.* **79**, 1431-1568.
Lu, Z. and Kipnis, J. (2010). Thrombospondin 1–a key astrocyte-derived neurogenic factor. *FASEB J.* **24**, 1925-1934.
Magnusson, J. P., Goritz, C., Tatarishvili, J., Dias, D. O., Smith, E. M. K., Lindvall, O., Kokaia, Z. and Frisen, J. (2014). A latent neurogenic program in astrocytes regulated by Notch signaling in the mouse. *Science* **346**, 237-241.
Matsa, E., Ahrens, J. H. and Wu, J. C. (2016). Human induced pluripotent stem cells as a platform for personalized and precision cardiovascular medicine. *Physiol. Rev.* **96**, 1093-1126.
Meamar, R., Nasr-Esfahani, M. H., Mousavi, S. A. and Basiri, K. (2013). Stem cell therapy in amyotrophic lateral sclerosis. *J. Clin. Neurosci.* **20**, 1659-1663.
Mine, Y., Tatarishvili, J., Oki, K., Monni, E., Kokaia, Z. and Lindvall, O. (2013). Grafted human neural stem cells enhance several steps of endogenous neurogenesis and improve behavioral recovery after middle cerebral artery occlusion in rats. *Neurobiol. Dis.* **52**, 191-203.
Morgan, P. J., Liedmann, A., Hübner, R., Hovakimyan, M., Rolfs, A. and Frech, M. J. (2012). Human neural progenitor cells show functional neuronal differentiation and regional preference after engraftment onto hippocampal slice cultures. *Stem Cells Dev.* **21**, 1501-1512.
Nedelec, S., Onteniente, B., Peschanski, M. and Martinat, C. (2013). Genetically-modified human pluripotent stem cells: new hopes for the understanding and the treatment of neurological diseases? *Curr. Gene Ther.*, **13**, 111-119.
Oki, K., Tatarishvili, J., Wood, J., Koch, P., Wattananit, S., Mine, Y., Monni, E., Tornero, D., Ahlenius, H., Ladewig, J. et al. (2012). Human-induced pluripotent stem cells form functional neurons and improve recovery after grafting in stroke-damaged brain. *Stem Cells* **30**, 1120-1133.
Pluchino, S., Quattrini, A., Brambilla, E., Gritti, A., Salani, G., Dina, G., Galli, R., Del Carro, U., Amadio, S., Bergami, A. et al. (2003). Injection of adult neurospheres induces recovery in a chronic model of multiple sclerosis. *Nature* **422**, 688-694.
Rybachuk, O., Kopach, O., Krotov, V., Voitenko, N. and Pivneva, T. (2017). Optimized model of cerebral ischemia in situ for the long-lasting assessment of hippocampal cell death. *Front Neurosci.* **11**, 388.
Sakata, H., Niizuma, K., Yoshioka, H., Kim, G. S., Jung, J. E., Katsu, M., Narasimhan, P., Maier, C. M., Nishiyama, Y. and et al. (2012). Minocycline-preconditioned neural stem cells enhance neuroprotection after ischemic stroke in rats. *J. Neurosci.* **32**, 3462-3473.
Shetty, A. K., Hattiangady, B. and Shetty, G. A. (2005). Stem/progenitor cell proliferation factors FGF-2, IGF-1, and VEGF exhibit early decline during the course of aging in the hippocampus: role of astrocytes. *Glia.* **51**, 173-186.
Staquicini, F. I., Dias-Neto, E., Li, J., Snyder, E. Y., Sidman, R. L., Pasqualini, R. and Arap, W. (2009). Discovery of a functional protein complex of netrin-4, laminin gamma1 chain, and integrin alpha6beta1 in mouse neural stem cells. *Proc. Natl. Acad. Sci. USA* **106**, 2903-2908.
Tornero, D., Tsupykov, O., Granmo, M., Rodriguez, C., Gronning-Hansen, M., Thelin, J., Smozhanik, E., Laterza, C., Wattananit, S., Ge, R. et al. (2017). Synaptic inputs from stroke-injured brain to grafted human stem cell-derived neurons activated by sensory stimuli. *Brain* **140**, 692-706.
Tsupykov, O., Kyryk, V., Smozhanik, E., Rybachuk, O., Butenko, G., Pivneva, T. and Skibo, G. (2014). Long-term fate of grafted hippocampal neural progenitor cells following ischemic injury. *J. Neurosci. Res.* **92**, 964-974.
Wurmser, A. E., Nakashima, K., Summers, R. G., Toni, N., D'amour, K. A., Lie, D. C. and Gage, F. H. (2004). Cell fusion-independent differentiation of neural stem cells to the endothelial lineage. *Nature* **430**, 350-356.
Zhou, F. W., Fortin, J. M., Chen, H. X., Martinez-Diaz, H., Chang, L. J., Reynolds, B. A. and Roper, S. N. (2015). Functional integration of human neural precursor cells in mouse cortex. *PLoS One* **10**, e0120281.